**The EMBO Journal** Vol. 22 No. 12 pp. 3175–3187, 2003

# The nuclear actin-related proteins Arp7 and Arp9: a dimeric module that cooperates with architectural proteins for chromatin remodeling

**Heather Szerlong, Anjanabha Saha and Bradley R.Cairns[1]**

Howard Hughes Medical Institute and Department of Oncological Sciences, Huntsman Cancer Institute, University of Utah School of Medicine, Salt Lake City, UT 84112, USA

[1]Corresponding author
e-mail: brad.cairns@hci.utah.edu

**Nuclear actin-related proteins (ARPs) are essential components of chromatin remodeling and modifying complexes, but their functions and relationship to actin remain elusive. The yeast SWI/SNF and RSC complexes contain Arp7 and Arp9, and are shown to form a stable heterodimer with the properties of a functional module. Arp7 and Arp9 rely on their actin-related regions for heterodimerization, and their unique C-termini cooperate for assembly into RSC. We suggest that regulated ARP–ARP (and possibly ARP–β–actin) heterodimerization might be a conserved feature of chromatin complexes. A RSC complex lacking Arp7/9 was isolated that displays robust nucleosome remodeling activity, suggesting a separate essential role for ARPs in the regulation of chromatin structure. A screen for suppressors of *arp* mutations yielded the DNA bending architectural transcription factor Nhp6, which interacts with RSC complex physically and functionally and shows facilitated binding to nucleosomes by RSC. We propose that Arp7/9 dimers function with DNA bending proteins to facilitate proper chromatin architecture and complex–complex interactions.**

*Keywords*: actin-related proteins/chromatin remodeling/nucleosome/Nhp6/RSC

## Introduction

Gene expression involves the modification and mobilization of nucleosomes, the fundamental unit of chromatin. Nucleosomes are mobilized by chromatin remodeling complexes (remodelers), which utilize the energy of ATP hydrolysis to alter DNA–histone contacts and reveal DNA elements recognized by transcription factors (Vignali *et al*., 2000; Havas *et al*., 2001; Saha *et al*., 2002). Remodelers work with nucleosome modifying complexes such as histone acetyltransferases (HATs), deacetylases and methyltransferases, which covalently modify nucleosomes and affect the association of additional factors, including remodelers (Narlikar *et al*., 2002). This process is dynamic and must be highly regulated, as interactions between remodelers and nucleosomes mediate transitions between the active and inactive conformations of chromatin.

There are four classes of remodeling complexes, ISWI, CHD/Mi-2, INO80 and SWI/SNF, defined by their different composition, *in vitro* activities and *in vivo* functions (Cairns, 1998; Boyer and Peterson, 2000; Havas *et al*., 2001). The SWI/SNF family consists of multiprotein complexes that are conserved from yeast to metazoans with central roles in gene regulation (Narlikar *et al*., 2002). *Saccharomyces cerevisiae* contains the founding member, SWI/SNF complex, and the highly related RSC (remodels the structure of chromatin) complex (Cairns *et al*., 1996). Likewise, human cells contain two highly related complexes, termed hSWI/SNF-A (also called BAF) and hSWI/SNF-B (also called PBAF) (Wang *et al*., 1996; Xue *et al*., 2000), whereas *Drosophila* utilize the single SWI/SNF-related Brm complex (Papoulas *et al*., 1998). All SWI/SNF-family complexes contain a DNA-dependent ATPase which serves as the 'engine' for nucleosome remodeling (Phelan *et al*., 1999; Saha *et al*., 2002) as well as several additional conserved proteins.

Intriguingly, all SWI/SNF remodelers also contain actin-related proteins (ARPs; Olave *et al*., 2002). ARPs constitute a large family of proteins present in all eukaryotes with important roles in both the nucleus and the cytoplasm (Schafer and Schroer, 1999; Machesky and May, 2001). *Saccharomyces cerevisiae* contains 10 ARPs (Arp1–Arp10), numbered by decreasing sequence similarity to actin, with Arp1 the most similar (Poch and Winsor, 1997). Importantly, recent structural studies suggest that new actin filaments are nucleated by the regulated heterodimerization of Arp2 and Arp3 (Robinson *et al*., 2001; Volkmann *et al*., 2001), and work presented here shows that heterodimerization is likewise required for Arp7/Arp9 function.

Nuclear ARP function involves chromatin structure, revealed first in genetic studies of epigenetic transcriptional regulation in yeast (Jiang and Stillman, 1996), and later through their biochemical identification as members of chromatin remodeling complexes (Cairns *et al*., 1998; Papoulas *et al*., 1998; Peterson *et al*., 1998; Zhao *et al*., 1998). Interestingly, all nuclear complexes that contain an ARP also contain either an additional ARP or actin itself, raising the possibility that nuclear ARPs (or ARP/actin) are paired physically. Yeast SWI/SNF and RSC contain both Arp7 and Arp9, two essential and non-redundant ARPs, whereas hSWI/SNF and *Drosophila* Brm complex contain one ARP (Baf53 in hSWI/SNF, BAP55 in *Drosophila*) and one molecule of β-actin. Remarkably, yeast INO80 complex contains three ARPs (Arp4, 5 and 8) and β-actin (Shen *et al*., 2000). An ARP is also present, along with β-actin, in HAT complexes such as the essential yeast H4 acetyltransferase complex NuA4 (Galarneau *et al*., 2000) and human TIP60 and related complexes (Ikura *et al*., 2000; Park *et al*., 2002), which have clear roles in activation by c-*myc*, apoptosis and DNA repair.

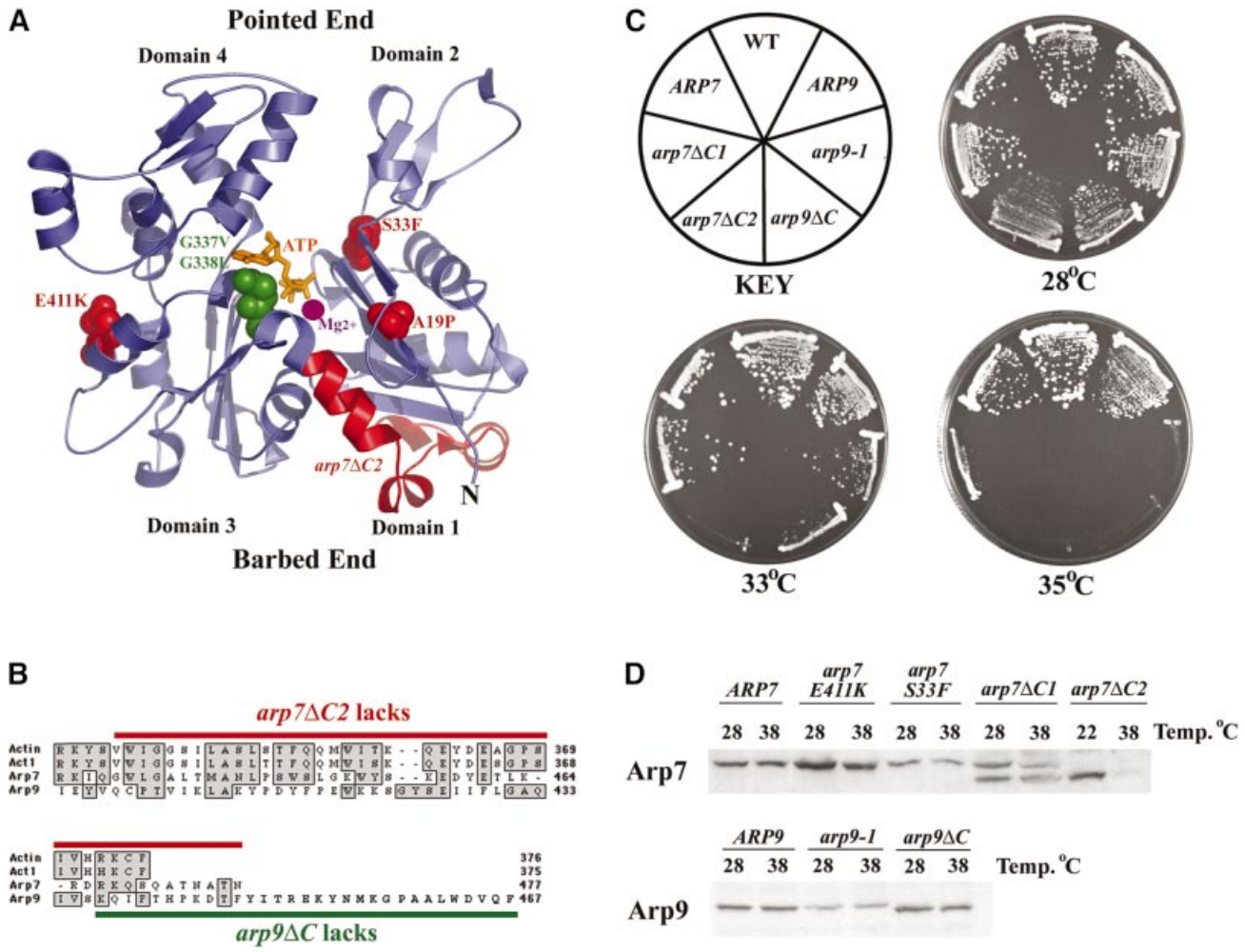


**Fig. 1.** New conditional mutations in *ARP7* and *ARP9*. (**A**) Mutations in *arp7* (red) and *arp9* (green) superimposed on the structure of actin (Kabsch *et al.*, 1990). (**B**) C-terminal regions lacking in *arp7* (red) or *arp9* (green) truncation alleles. Regions of similarity are boxed in grey. Rabbit actin (top row). (**C**) Growth of Ts⁻ *arp7* and *arp9* strains. Strains given below. (**D**) Protein expression profiles of *arp* proteins. Whole-cell extracts from WT and Ts⁻ *arp* strains grown at the temperatures indicated were immunoblotted with either polyclonal anti-Arp7 or anti-Arp9 antibody. Strains: pNCT.*ARP7* (YBC1533), pNCT *arp7E411K* (YBC776), pNCT.*arp7S33F* (YBC788), pNCT.*arp7ΔC1* (YBC786), pNCT.*arp7ΔC2* (YBC1534); for *ARP9*, pNCT.*ARP9* (YBC1535), pNCT.*arp9-1* (YBC1536) or pNCT.*arp9ΔC* (YBC775). Wild type (WT) (YBC605).

At present, we understand little about nuclear ARP or actin function; however, studies on cytoplasmic actin and the Arp2/3 complex may serve as a guide. Structurally, actin is an ATPase that is divided into four domains (Kabsch and Holmes, 1995) (Figure 1A). The central sections of domains 1 and 3 combine to form the central 'actin fold', which is important for actin structure and ATPase activity. The outer regions of domains 1 and 3 combine to form the barbed end, where monomer addition occurs, whereas domains 2 and 4 combine to form the pointed end. ARPs are highly similar to actin in the central actin fold, but show less conservation in peripheral regions (Robinson *et al.*, 2001), suggesting specialization of interactions. In addition, all ARPs contain either internal 'loop' insertions or C-terminal extensions (unique to each ARP) that may confer additional specialized functions. Indeed, one loop insertion unique to yeast Arp4 is highly acidic, and can interact with all four histones regardless of acetylation state (Harata *et al.*, 1999; Galarneau *et al.*, 2000). The region within the actin fold serves two functions in actin: protein structure and ATP hydrolysis. However, genetic evidence suggests that Arp7 and Arp9 are similar to actin structurally but lack ATP hydrolysis or binding (Cairns *et al.*, 1998).

Here we take both biochemical and genetic approaches to understand Arp7 and Arp9 function. We identify the architectural transcription factor *NHP6A* (non-histone protein 6) as a multicopy suppressor of *arp7* and *arp9* conditional alleles. Nhp6a has demonstrated roles in both transcriptional initiation and elongation and may alter DNA structure to promote appropriate promoter architecture and enable co-complex formation or recruitment (Paull *et al.*, 1996; Formosa *et al.*, 2001). Interestingly, an HMG-D domain similar to that in Nhp6 is present in the hSWI/SNF component Baf57 (Wang *et al.*, 1998) and the *Drosophila* Brm complex component BAP111 (Papoulas *et al.*, 2001), raising the possibility that Nhp6 may perform a related function in RSC or SWI/SNF. Our work suggests that ARP heterodimers work with HMG proteins to facilitate proper chromatin architecture.

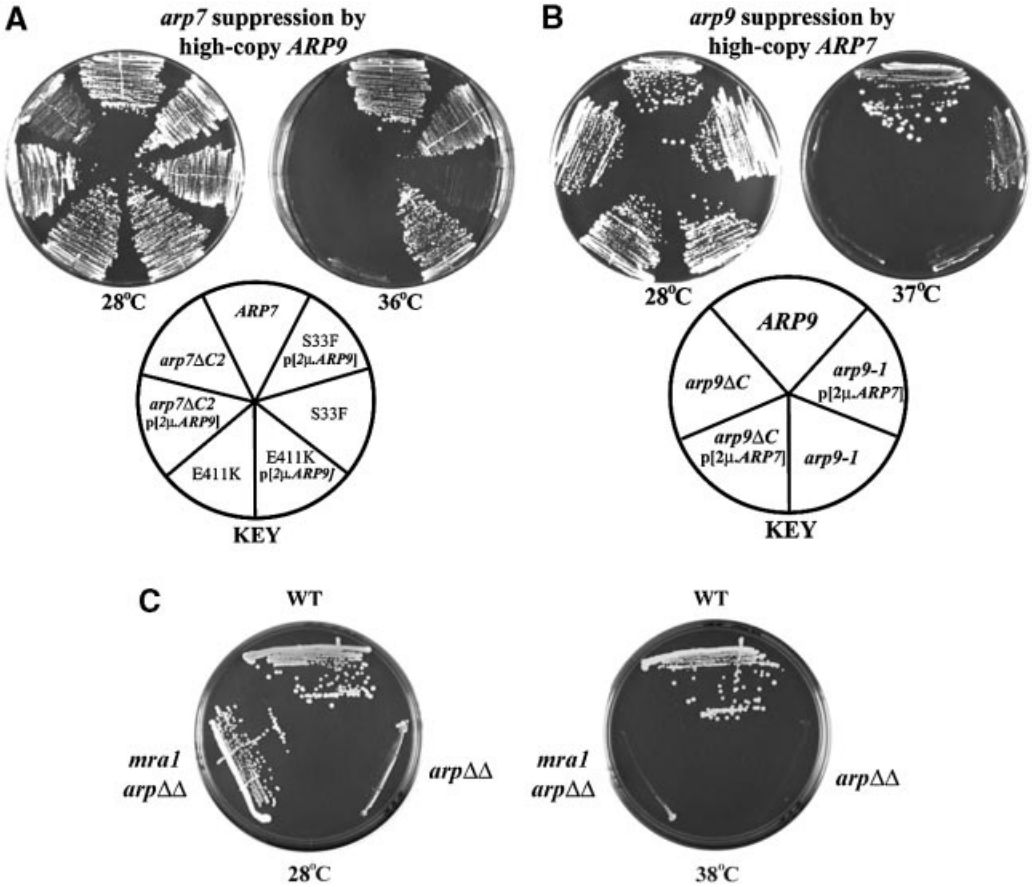


**Fig. 2.** *ARP7* and *ARP9* cosuppression relationships and suppression by *mra1*. (**A**) Suppression of *arp7* mutations by multicopy *ARP9*. Strains: WT pNCT.ARP7 (YBC1533). *arp7* Ts⁻ alleles: pNCT.*arp7S33F* (YBC788), pNCT *arp7E411K* (YBC776), pNCT.*arp7ΔC2*(YBC1534). Growth of WT and *arp7* Ts⁻ strains transformed with either YEp24.*ARP9* or YEp24 alone on SC-Ura at 28°C or 36°C. (**B**) Suppression of *arp9* mutations by multicopy *ARP7*. Growth of WT and *arp9* Ts⁻ strains transformed with either YEp24.*ARP7* or YEp24 alone on SC-Ura at 28°C or 37°C. Strains: WT (YBC1535), pNCT.*arp9-1* (YBC1536) and pNCT.*arp9ΔC* (YBC775). (**C**) *mra1* is a suppressor of *arp7*Δ and *arp9*Δ mutations. All W303 background: WT (BCY405), *arp9*Δ *arp7*Δ (BCY393) and the triple *arp9*Δ *arp7*Δ *mra1-1* (BCY395) were compared for growth on rich media plates at 30°C or 38°C.

## Results

### *Isolation and characterization of new alleles of arp7 and arp9*

We previously isolated temperature sensitive (Ts⁻) mutations in *arp7* including A19P, S33F, E411K and G396V (Cairns *et al*., 1998), and here we isolate and characterize new conditional missense and nonsense (truncation) mutations in *ARP7* and *ARP9*. Arp7 and actin are similar within the actin fold, allowing *arp7* missense mutations in this region to be superimposed on the actin structure (Kabsch *et al.*, 1990; Cairns *et al*., 1998), providing an estimate of their relative locations (Figure 1A). The *arp7* nonsense allele *arp7ΔC1* places a stop codon at position 436, truncating 42 amino acids (Figure 1B). However, *arp7ΔC1* encoded two protein species, the truncated Arp7ΔC1 protein as well as full-length Arp7 (Figure 1D), due to nonsense suppression (data not shown). To produce only the truncation $Arp7_{1–435}$, we inserted two stop codons, resulting in *arp7ΔC2*. Strains bearing *arp7ΔC2* contained only $Arp7_{1–435}$, and grew well at 22°C and slowly at 28°C, and were unable to grow at 35°C (Figure 1C) likely due to the instability of $Arp7_{1–435}$ at higher temperatures (Figure 1D).

The *arp9* nonsense mutation described previously (*arp9-661*, now renamed *arp9ΔC*) lacks the C-terminal 30 amino acids, $Arp9_{1–437}$ (Figure 1B) and produces a stable truncated product as well as a very low level of full-length protein due to nonsense suppression (Figure 1D and data not shown). However, a strain bearing an *arp9* derivative (bearing two stop codons) encoding only $Arp9_{1–437}$ was nonviable at all temperatures (data not shown), suggesting that *arp9ΔC* viability relies on the small amount of full-length Arp9 protein produced. Taken together, the C-terminal 30 amino acids of Arp9 are essential for viability whereas the C-terminal 42 amino acids of Arp7 are required for growth and protein stability at high temperature. As these C-termini lack homology to actin, they may represent domains with unique functions, and their roles are determined below.

Prior screens did not yield missense mutations in *ARP9* that conferred temperature sensitivity. They were obtained here by using *arp7*G396V as a guide and targeting the equivalent region in *ARP9* using a library of mutagenic oligonucleotides, yielding the double substitution G337V G338L (termed *arp9-1*). Strains bearing *arp9-1* grew well at 28°C and produced a protein product within about 2-fold of wild-type Arp9 (Figure 1D) but lacked growth

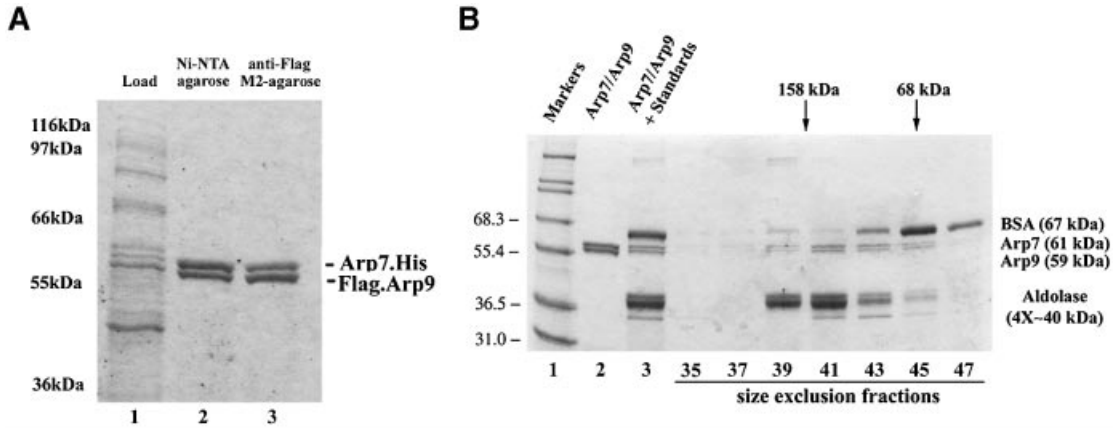


**Fig. 3.** Purification and characterization of a stable Arp7–Arp9 heterodimer. (**A**) Arp7 and Arp9 copurify. Histidine-tagged Arp7 and Flag-tagged Arp9 were coexpressed in *E.coli* using a bi-cistronic vector (lane 1). Soluble protein extracts were subjected to tandem affinity purification using Ni-NTA resin (lane 2) followed by anti-Flag resin (lane 3). Samples were separated in a 7.5% acrylamide–SDS gel and visualized by staining with Coomassie Blue dye. (**B**) Gel filtration chromatography reveals an Arp7–Arp9 heterodimer. Arp7–Arp9 complex eluted from Ni-NTA (lane 2) was combined with the size standards bovine serum albumin (BSA) and aldolase (lane 3) and separated on a Superdex-200 column. Samples were separated in a 7.5% acrylamide–SDS gel and visualized with Coomassie Blue.

ability at 35°C (Figure 1C). Thus, we have isolated point mutations and C-terminal truncation mutations in both *ARP7* and *ARP9* that are suitable for subsequent genetic and biochemical analysis.

### Cosuppression relationships provide genetic evidence for Arp7/Arp9 interaction

As Arp7 and Arp9 are the only shared components between RSC and SWI/SNF complexes, they may interact physically as a functional module. If so, mutations in one ARP that impair interactions between the two ARPs might be suppressed by increased dosage of the partner ARP. We find that increased dosage of *ARP9* suppresses the temperature sensitivity of the *arp7* missense strains tested, including *arp7E411K* and *arp7S33F* (also *arp7A19P*, data not shown), but is largely ineffective with *arp7ΔC2* (Figure 2A). Likewise, increased dosage of *ARP7* suppresses the temperature sensitivity of an *arp9-1* strain, but not an *arp9ΔC* strain (Figure 2B). These results suggest that conditional mutations in the actin fold impair Arp7/9 interaction.

### Arp7 and Arp9 form a stable heterodimer

To test more directly whether Arp7 and Arp9 interact physically, we tested for copurification of recombinant derivatives using a bi-cistronic coexpression system in *Escherichia coli*. Here, Arp7 was tagged with seven histidines at its C-terminus and Arp9 was tagged with the Flag epitope at its N-terminus. Whereas expression of either ARP in isolation led to largely (Arp9) or entirely (Arp7) insoluble protein (data not shown), coexpression rendered both largely soluble. Arp7 and Arp9 copurified using either Ni-NTA resin (specific for the histidine tag) or with anti-Flag M2 resin, were resistant to high salt (600 mM KCl), and were obtained in high yield and purity (Figure 3A). Size exclusion chromatography revealed a complex of ~140 kDa, only slightly larger than the 120 kDa estimated for a spherical Arp7/Arp9 heterodimer (Figure 3B). Arp7 and Arp9 appeared stoichiometric in the purified material, as estimated from staining intensity. Taken together, Arp7 and Arp9 form a stable heterodimeric complex and represent the first purification of an isolated ARP/ARP heterodimer.

### mra1 suppresses arp7 and/or arp9 null mutations

Rigorous testing of Arp7 and Arp9 function requires the analysis of RSC or SWI/SNF complexes lacking Arp7 and Arp9 both *in vivo* and *in vitro*. However, *ARP7* and *ARP9* are each essential genes in the common S288C genetic background, and nearly essential in the common W303 genetic background (Cairns *et al*., 1998). However, we isolated spontaneous suppressors of *arp7Δ*, *arp9Δ* or *arp7Δ arp9Δ* mutants at very low frequency in W303 strains, (termed *mra1-1*, *mra1-2* and *mra1-3*, respectively), as they modify the requirement for actin-related proteins (data not shown).

All three *mra1* alleles suppressed the single or double *arpΔ* null mutations equally well and all three were tightly linked, strongly suggesting a single locus (data not shown). These *mra1* mutations restored near-wild-type growth ability on rich media plates at 28°C (Figure 2C). However, *mra1* confers only partial suppression of *arpΔ* mutations, as *mra1 arpΔ* double mutants still displayed an exceptionally wide variety of strong phenotypes such as the inability to grow on raffinose or sucrose, or on plates lacking inositol, all known phenotypes of *swi/snf* mutants. These double mutants additionally displayed *rsc* mutant phenotypes, including marked sensitivity to temperature, formamide and caffeine, and high osmolarity (Figure 2C; data not shown). However, these growth defects are attributable to the *arp* mutation, as *mra1* mutations in isolation (otherwise WT) did not confer any detectable phenotype, which has prevented our identification of the gene. Regardless, viable *mra1 arpΔ* mutants enable the isolation of RSC complex lacking Arp7 and Arp9, and the ability to analyze the activity and assembly properties of these complexes.

### Arp7 and Arp9 are obligate partners in RSC and SWI/SNF complexes in vivo

To determine whether Arp7/9 heterodimerization is required for assembly into RSC or SWI/SNF, we per-

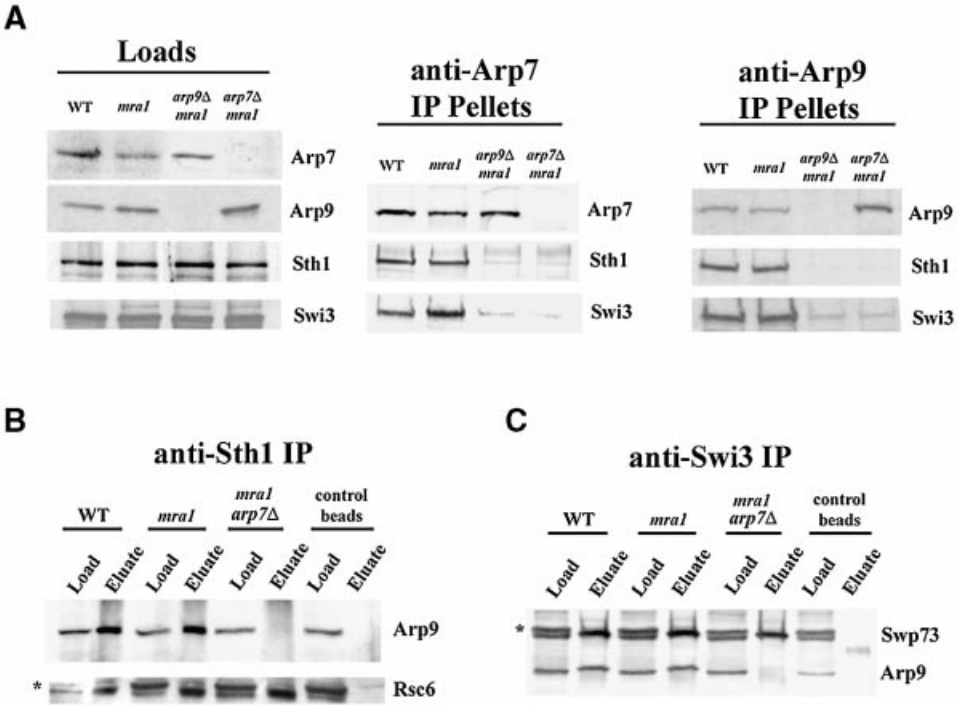


**Fig. 4.** Arp7 and Arp9 are obligate partners *in vivo*. (**A**) Arp7 and Arp9 codependence for assembly into RSC or SWI/SNF complexes. Extracts were prepared from WT (YBC405), *mra1* (YBC430), *mra1 arp9*Δ (YBC426) and *mra1 arp7*Δ (YBC427) strains (left panel). Immune complexes were formed with anti-Arp7 (middle panel) or anti-Arp9 (right panel), washed, eluted, immunoblotted and probed with anti-Sth1 or anti-Swi3 antiserum. Assembly defects of Arp9 in *arp7*Δ mutants in (**B**) RSC or (**C**) SWI/SNF. Whole-cell extracts from WT (YBC405), *mra1* (YBC430) and *mra1 arp7*Δ (YBC427) were prepared (Loads). Immune complexes were formed with (B) anti-Sth1 or (C) anti-Swi3, washed, eluted, immunoblotted and probed with anti-Arp9 antiserum or antiserum specific for subunits of RSC (Rsc6) or SWI/SNF complex (Swp73) as controls. *Anti-Rsc6 and anti-Swp73 antibodies each cross react with a protein of slightly higher molecular weight. However, only the faster migrating species (bona fide Rsc6 or Swp73) is coprecipitated, providing an internal control for specificity.

formed co-immunoprecipitation experiments using *arp*Δ *mra1* strains. Assembly into RSC was monitored by association of ARPs with Sth1 or Rsc6, whereas assembly into SWI/SNF was determined by association with Swi3 or Swp73. Arp7 required Arp9 for assembly into RSC or SWI/SNF, as anti-Arp7 coprecipitated Sth1 or Swi3 from extracts derived from wild-type (WT) or *mra1* strains, but not from an *mra1 arp9*Δ strain (Figure 4A). Likewise, Arp9 required the presence of Arp7 to associate with RSC or SWI/SNF components, as anti-Arp9 did not coprecipitate Sth1 or Swi3 from an *mra1 arp7*Δ strain (Figure 4A). The reciprocal set of experiments using anti-Sth1 (Figure 4B) or anti-Swi3 (Figure 4C) verified these results (Arp7, data not shown). Taken together, these experiments suggest that Arp7 and Arp9 must heterodimerize to assemble into RSC or SWI/SNF complexes.

### *Purification of a RSC complex lacking Arp7 and Arp9*

A RSC complex lacking Arp7 and Arp9 (RSCΔ7/9) was isolated from an *arp7*Δ *arp9*Δ *mra1* strain, which harbored a plasmid encoding a TAP-tagged [Tandem Affinity Purification (Puig *et al*., 2001)] form of Rsc2 useful for protein purification. Purification at high stringency followed by staining with silver revealed an RSCΔ7/9 complex that appeared to lack only Arp7 and Arp9, and no new additional proteins were detected (Figure 5A and B).

### *RSC complex lacking Arp7 and Arp9 displays robust ATPase and nucleosome remodeling activities*

Current models for ARP function include regulation of DNA-dependent ATPase activity, remodeling activity or nucleosome binding (Harata *et al*., 1999; Boyer and Peterson, 2000; Olave *et al*., 2002). Therefore, RSCΔ7/9 was tested for DNA-dependent ATPase activity, DNA translocation and mononucleosome binding and remodeling. The isolated ATPase 'engines' of the remodelers RSC or hSWI/SNF (Sth1 or human Brg1, respectively) display only ~15% of the nucleosome remodeling activity observed with RSC (or hSWI/SNF) complex (Phelan *et al*., 1999; Saha *et al*., 2002), raising the possibility that ARP proteins could contribute to remodeling efficiency. However, RSCΔ7/9 was nearly identical to WT RSC in ATP turnover values for double-stranded DNA (5.9 versus 6.3 ATP/s, respectively; data not shown). Likewise, WT RSC and RSCΔ7/9 function nearly identically (within 15%) in a triple-helix displacement assay (used to monitor DNA translocation) (Figure 5C), and were essentially equally effective in a mononucleosome remodeling assay (tested in conditions of limiting enzyme) involving the ATP-dependent accessibility of a *Dra*I restriction endonuclease site present on a mononucleosome (Figure 5D). The purified Arp7/9 dimer showed no interaction with recombinant (and unmodified) mononucleosomes over a wide concentration range (1–400 molar excess; data not

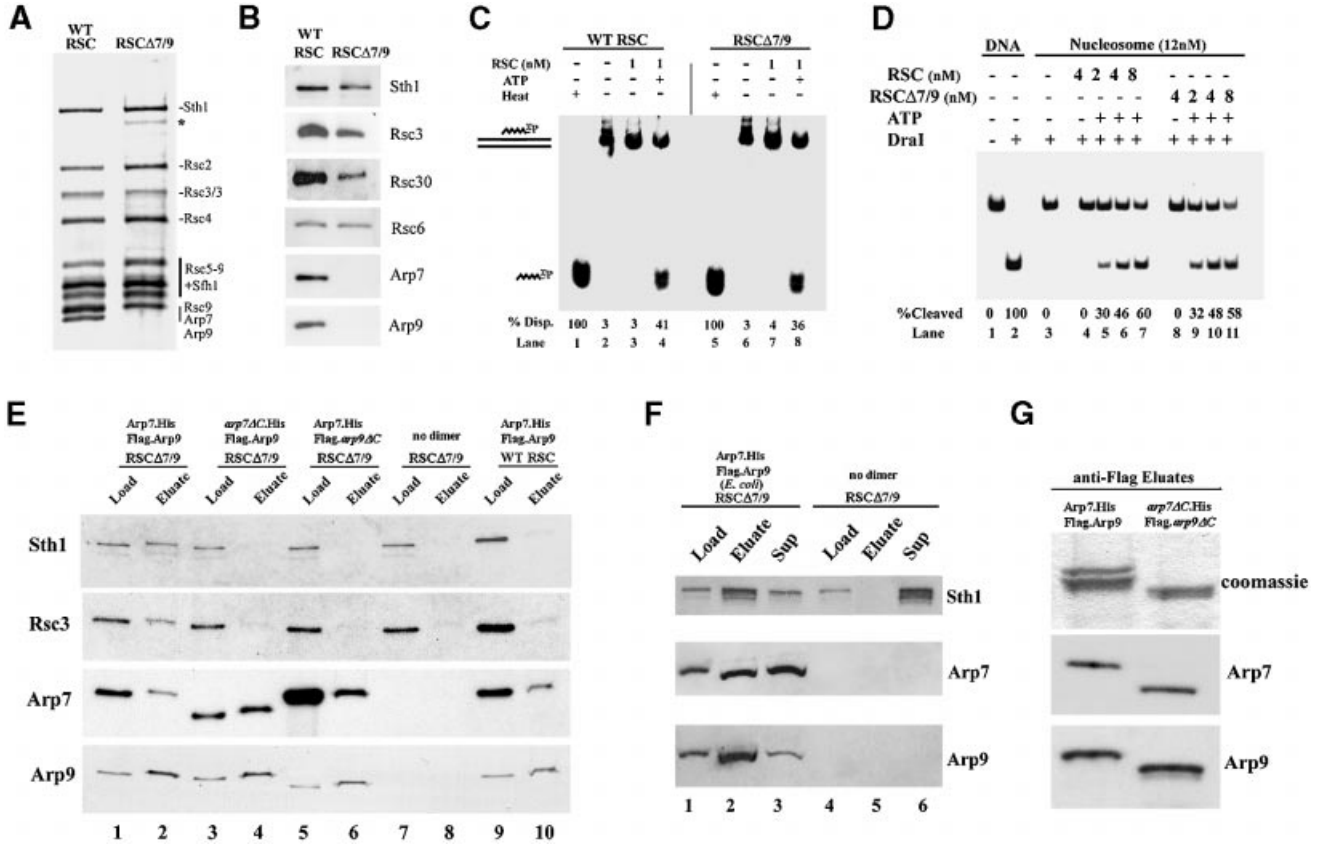


**Fig. 5.** Composition and activity of RSC lacking Arp7 and Arp9. (**A**) Purification of RSCΔ7/9, a stable RSC complex lacking Arp7 or Arp9. RSC and RSCΔ7/9 were purified (see Materials and methods), and 600 ng of each was separated on a 7.5% acrylamide–SDS gel, followed by staining with silver. *A low-level degradation product of Sth1. (**B**) Immunoblot analysis of RSCΔ7/9. Purified RSC (125 ng) or RSCΔ7/9 (125 ng) was separated in a 7.5% acrylamide–SDS gel and immunoblotted with antiserum raised against Sth1, Rsc3, Rsc30, Rsc6, Arp7 or Arp9. (**C**) RSCΔ7/9 displaces a triple helix. A triple-helix substrate consisting of a 40-base triple-helical region was centered on a 190 bp duplex DNA, treated as indicated for 60 min at 30°C or heated briefly at 90°C (Heat) and separated in a 15% polyacrylamide gel. Displacement of the $^{32}$P-labeled third strand as a percentage of total (%Disp.) was quantified with Image Quant. (**D**) RSCΔ7/9 remodels mononucleosomes efficiently. Recombinant yeast octamers were assembled into mononucleosomes (172 bp 5S DNA, $^{32}$P-end labeled) containing a single *Dra*I site near the dyad and purified. Reaction components: RSC or RSCΔ7/9 (as indicated); nucleosomes (12 nM); ATP (1 mM); *Dra*I (20 units). Conditions: 1 h at 30°C, followed by DNA extraction, separation and autoradiography. (**E**) Reconstitution of the yeast Arp7/Arp9 heterodimer with RSCΔ7/9 and the requirement for the C-termini of Arp7 and Arp9 for assembly into RSC. Arp7/9 heterodimer derivatives were expressed and purified, normalized for Arp9 content, bound to anti-Flag M2 agarose, washed (200 mM NaCl), incubated with RSCΔ7/9 (4:1 molar ratio of Arp7/9 to RSC), washed (500 mM NaCl) and eluted with Flag peptide. Immunoblot analysis of RSC reconstitutions. L: load, 10% of total. E: eluate, 40%. (**F**) A recombinant (*E.coli*) Arp7/9 dimer reconstitutes into RSC. Purified Arp7/9 dimer from *E.coli* was bound to anti-Flag M2 agarose and treated as in (E). (**G**) Recombinant Arp7ΔC and Arp9ΔC copurify. Histidine-tagged Arp7ΔC (1–435) and Flag-tagged Arp9ΔC (1–437) were coexpressed in *E.coli* using a bi-cistronic vector and purified as described in Figure 3 and Materials and methods. Arp7ΔC and Arp9ΔC migrate at nearly the identical position.

shown). Thus, Arp7 and Arp9 likely have essential roles that are distinct from the basic remodeling mechanism.

### *Reconstitution of RSC and the requirement for Arp7/9 carboxyl termini*

To determine whether the Arp7/9 C-termini connect the Arp7/9 heterodimer to the RSC complex, we developed a RSC reconstitution assay. We coexpressed full-length ARP proteins or those lacking a C-terminus in yeast, purified the corresponding heterodimer using the Arp7 histidine tag (data not shown) and utilized the Arp9 Flag tag for immobilization on anti-M2 Flag agarose beads. Immobilized Arp7/9 heterodimer derivatives were incubated with either purified RSCΔ7/9 or pure WT RSC, washed at high (500 mM NaCl) stringency and eluted with Flag peptide to release associated proteins. RSC could be reconstituted on the bead from RSCΔ7/9 and full-length Arp7/9 heterodimer, whereas WT RSC (containing Arp7/9) did not interact (Figure 5E). The C-termini of both Arp7 and Arp9 were required for assembly into RSC, suggesting that their C-termini cooperate for assembly. In addition, the individual C-termini of Arp7 and Arp9 are not required for heterodimerization, as the truncated Arp7/9 heterodimers could be purified and remained stably associated during the high stringency wash (Figure 5E). Arp7/9 heterodimers purified from *E.coli* also assemble efficiently into RSCΔ7/9, verifying that no other yeast protein is required for assembly in this assay (Figure 5F). Furthermore, derivatives lacking both C-termini (Arp7ΔC, 1–435; Arp9ΔC, 1–437) expressed in *E.coli* are stably associated, showing that the actin-related regions are sufficient for interaction (Figure 5G). Finally, derivatives lacking either tail assemble poorly into RSC *in vivo*, as precipitation of RSC (anti-Sth1) from extracts at moderate stringency (250 mM NaCl) fails to coprecipitate Arp7/9 truncation derivatives (data not shown).

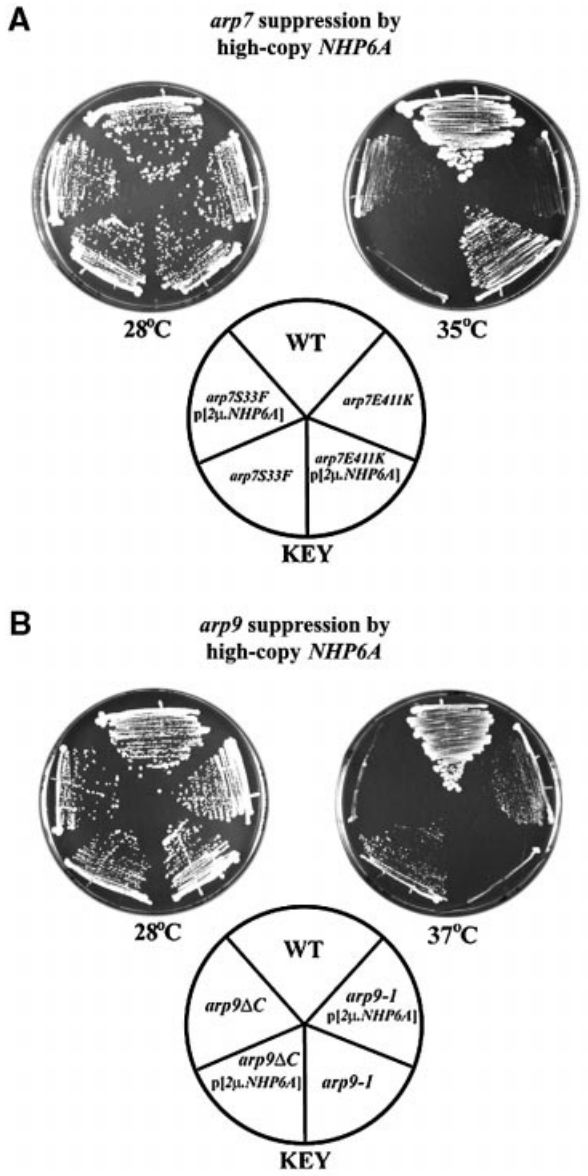


**Fig. 6.** Multicopy *NHP6A* suppresses *arp* alleles. (**A**) Suppression of *arp7* Ts⁻ alleles by multicopy *NHP6A*. Plasmid YEplac195 *NHP6A* or empty vector were transformed into WT or the *arp7* Ts⁻ strains and grown at 28°C or 35°C. Strains: YBC726 transformants harboring WT pNCT.ARP7 or plasmids bearing *arp7* Ts⁻ alleles: pNCT.*ARP7* (YBC1533), pNCT *arp7E411K* (YBC776) or pNCT.*arp7S33F* (YBC788). (**B**) Suppression of *arp9* Ts⁻ alleles by multicopy *NHP6A*. YEplac195 *NHP6A* plasmid or empty vector were transformed into WT or *arp9* Ts⁻ strains and compared for growth at 28°C or 37°C. Strains: YBC86 transformants harboring pNCT.*ARP9* (YBC1535), pNCT.*arp9-1*(YBC1536) or pNCT. *arp9ΔC* (YBC775).

### *arp7 and arp9 mutations are suppressed by increased dosage of NHP6A/B*

To understand better the function of the Arp7/Arp9 heterodimer, we selected for suppressors of the temperature sensitivity conferred by the *arp7-122* (E411K) missense mutation using a multicopy plasmid library. Plasmids directing strong suppression all contained *ARP7* or *ARP9*, which were obtained twice and 11 times, respectively. One genomic fragment directing moderate suppression contained *NHP6A*, and multicopy *NHP6A* alone was equally effective in restoring growth ability of *arp7E411K* at 35°C (Figure 6A; data not shown). In addition, increased dosage of the nearly identical gene *NHP6B* was somewhat less effective, enabling slow growth at 36°C (data not shown). Multicopy *NHP6A* suppressed all *arp7* alleles tested except the truncation allele *arp7ΔC2* (Table I), probably due to the instability and absence of Arp7 protein encoded by *arp7ΔC2* at high temperature (Figure 1D). In addition, both the missense allele *arp9-1* and the truncation allele *arp9ΔC* were partially suppressed (Figure 6B and Table I). Importantly, high-copy *NHP6A* cannot suppress *arp7Δ* or *arp9Δ* mutants (in W303 background, Table I) or other *rsc* alleles tested, and actually *inhibits* the growth of WT strains, further suggesting that the suppression of *arp7* or *arp9* mutations is significant.

### *Combining rsc or swi/snf mutations with nhp6a nhp6b mutations causes increased sickness or lethality*

As increased dosage of *NHP6A/B* may improve *arp7/9* mutant growth ability; conversely, the absence of *NHP6A/B* impairs *arp7/9* growth ability. *NHP6A* and *NHP6B* are largely redundant, as phenotypes such as temperature sensitivity require a double *nhp6a nhp6b* (*nhpΔΔ*) null mutation (Costigan *et al*., 1994). Combining *nhpΔΔ* mutations with *arp9ΔC* or *arp9-1* resulted in lethality or extremely slow growth, respectively, at temperatures permissive for each of the parent strains (Table II). In contrast, *nhpΔΔ* combined with either *snf2Δ* or alleles of *sth1* (*sth1-2 and sth1-3*) were viable, though a slight lowering of the restrictive temperature was observed. In addition, *nhpΔΔ* combinations with *rsc9-1 or snf2Δ* resulted in a lowering of the semi-permissive temperature (Table II). Taken together, we observe strong genetic interactions between *nhp6* mutations and *arp9* mutations, and weaker interactions with other mutations in RSC and SWI/SNF components, again suggesting that the functional interaction involves these complexes in general but is more closely linked to ARP function.

### *A small proportion of Nhp6a is physically associated with RSC*

To determine whether RSC and Nhp6 interact physically we performed co-immunoprecipitation experiments, and found that a small proportion (about 1%) of Nhp6a protein stably associated with RSC under moderately high (250 mM NaCl) salt conditions and was unaffected by DNase treatment (Figure 7A and B). This estimate (1%) is a conservative lower limit based on IP efficiency and comparison with input. These results are consistent with a recent genome-wide TAP tagging experiments, which revealed RSC components in association with Nhp6b (as well as 24 other candidate interacting factors) at low stringency conditions (150 mM NaCl) (Gavin *et al*., 2002). Interestingly, Nhp6 interacts with RSC in extracts prepared from *mra1 arp7Δ arp9Δ* strains, showing that Arp7 and Arp9 cannot constitute the sole interaction surface, or possibly that *mra1* improves interaction of RSC with Nhp6 (Figure 7B). Taken together, these results show that Nhp6a interacts with a small portion of RSC physically and with Arp7/9 functionally.

**Table I.** *arp7* and *arp9* mutations are suppressed by increased dosage of *NHP6A*

| Genotype | Growth with multicopy empty vector | Growth with multicopy NHP6A | Temperature (°C) | Strain[a] |
|---|---|---|---|---|
| WT | +++ | ++ | 28–38 | YBC605 |
| *ARP7* | | | | |
| *arp7Δ* | – | – | 28 | BCY366 |
| *arp7E114K* | – | ++ | 35 | YBC776 |
| *arp7A19P* | – | + | 35 | YBC787 |
| *arp7S33F* | – | + | 35 | YBC788 |
| *arp7G330R* | – | + | 38 | YBC778 |
| *arp7ΔC2* | – | – | 33 | YBC1534 |
| *ARP9* | | | | |
| *arp9Δ* | – | – | 28 | BCY330 |
| *arp9-1* | – | + | 37 | YBC1536 |
| *arp9*ΔC | – | + | 37 | YBC775 |
| *sth1BDΔHA* | + | + | 38 | YBC1196 |
| *rsc2Δ* | ++ | + | 38 | YBC79 |
| *RSC3* | | | | |
| *rsc3-1* | – | – | 38 | YBC840 |
| *rsc3-2* | – | – | 38 | YBC842 |
| *rsc3-3* | – | | 38 | YBC906 |
| *RSC8* | | | | |
| *swh3-ΔC* | – | – | 38 | YBC1552 |
| *swh3-ts21* | – | – | 33 | YBC1551 |
| *rsc9-1* | – | – | 33 | YBC1156 |

[a]BCY strains and YBC strains are derivatives of the W303 and S288C genetic backgrounds, respectively.
+++, WT growth; ++, slow growth; +, very slow growth; –, no growth.

**Table II.** Combining *rsc* or *swi/snf* mutations with *nhp6a nhp6b* mutations causes increased sickness or lethality

| *rsc* allele | *nhp6* allele | Growth at 28°C | NPT[a] (°C) | Strain[b] |
|---|---|---|---|---|
| *WT* | *NHP6A/B* | +++ | >38 | YBC605 |
| *WT* | *nhp6ΔΔ* | ++ | 38 | YBC1304/1305/1307 |
| *arp9-1* | *NHP6A/B* | +++ | 35 | YBC1536 |
| *arp9-1* | *nhp6ΔΔ* | + | 33 | YBC1526 |
| *arp9ΔC* | *NHP6A/B* | ++ | 35 | YBC775 |
| *arp9ΔC* | *nhp6ΔΔ* | – | 28 | YBC1525 |
| *sth1-2 (P646L)* | *NHP6A/B* | +++ | >38 | YBC946 |
| *sth1-2 (P646L)* | *nhp6ΔΔ* | ++ | 35 | YBC1520 |
| *sth1-3 (S806L,T881M)* | *NHP6A/B* | +++ | >38 | YBC944 |
| *sth1-3 (S806L,T881M)* | *nhp6ΔΔ* | + | 35 | YBC1517 |
| *rsc9-1* | *NHP6A/B* | ++ | 33 | YBC1158 |
| *rsc9-1* | *nhp6ΔΔ* | + | 33 | YBC1621 |
| *swi/snf* allele | | | | |
| *snf2Δ* | *NHP6A/B* | +++ | >38 | YBC27 |
| *snf2Δ* | *nhp6ΔΔ* | ++ | 35 | YBC1514 |

[a]NPT; non-permissive temperature.
[b]All strains are derivatives of the S288C genetic background.
+++, WT growth; ++, slow growth; +, very slow growth; –, no growth.

### *RSC facilitates the binding of Nhp6a to nucleosomal DNA*

Remodelers bind nucleosomes and enable the binding of factors to nucleosomal DNA through ATP-dependent alteration of nucleosomal DNA topology. We find that the combination of RSC and ATP promotes the association of Nhp6a with the nucleosome, providing an Nhp6-NUC complex at low concentrations of Nhp6a (Figure 7C, compare lanes 5 and 6 with lanes 13 and 14). Here, RSC action probably results in the exposure of nucleosomal DNA, followed by binding of Nhp6a and then release of the Nhp6-NUC complex by RSC. Interestingly, the loading of Nhp6a is correlated with the loss of *Dra*I restriction site accessibility on the nucleosome (Figure 7D). Nhp6a has no effect on RSC ATPase activity or on *Dra*I activity on naked DNA (data not shown), and has only a slight effect on nucleosomal ATPase activity (Figure 7D, when nucleosomes are limiting), suggesting that this inhibition involves a particular aspect of nucleosome remodeling (see Discussion). These results show that RSC helps load Nhp6a onto nucleosomal DNA, and suggests that factor loading can affect the accessibility of other sites on the nucleosome and/or inhibit a specific aspect of the remodeling process.

## Discussion

Nuclear ARPs are essential components of several chromatin remodeling and modifying complexes; however, their functions in these complexes are largely unknown. Here, we provide four new insights into nuclear ARP function. First, Arp7 and Arp9 are obligate heterodimers both physically and functionally, a result which takes on greater significance in light of the recent discovery that Arp2/Arp3 heterodimerization controls actin filament formation in the cytoplasm. Secondly, Arp7/Arp9 heterodimerization relies on their actin-related region, which then enables their C-terminal extensions to coordinate their assembly into RSC complex. Thirdly, Arp7 and Arp9 are not required for many of the activities previously proposed for ARPs, including DNA-dependent ATPase activity, DNA translocation activity or mononucleosome binding or remodeling. Fourthly, the architectural transcription factor Nhp6a interacts with RSC physically and with Arp7 and Arp9 functionally, and may provide an HMG-related function to RSC that is analogous to mammalian BAF57. Importantly, we further show that RSC helps load Nhp6a onto nucleosomal DNA and that such loading affects subsequent nucleosomal access. Together, these results reveal new physical and functional contexts for ARP and Nhp6 function.

### *Nuclear ARPs as heterodimeric modules*

Our results suggest that assembly of Arp7/9 into RSC may involve two steps: heterodimerization, followed by C-terminal cooperativity for assembly. Recently, a crystal structure of the 'inactive' form of the Arp2/3 complex (lacking WASP) was solved (Robinson *et al*., 2001) in which Arp2 and Arp3 are not physically dimerized. However, a regulated conformational change is speculated to bring Arp2 and Arp3 together into the 'active' heterodimer configuration (May, 2001; Robinson *et al*., 2001) shown in electron micrograph images of Arp2/3 complex bound to branched filaments (Volkmann *et al*., 2001). Thus, ARP/ARP dimerization may be a conserved feature of ARP function, but utilized for different purposes in the nucleus and cytoplasm. Metazoan SWI/SNF complexes contain one ARP (Baf53) and actin itself, and this configuration is also found in HAT complexes in human cells (Baf53/actin) and yeast (Arp4/actin) (Olave *et al*., 2002). We speculate that actin/Baf53 (or actin/Arp4)

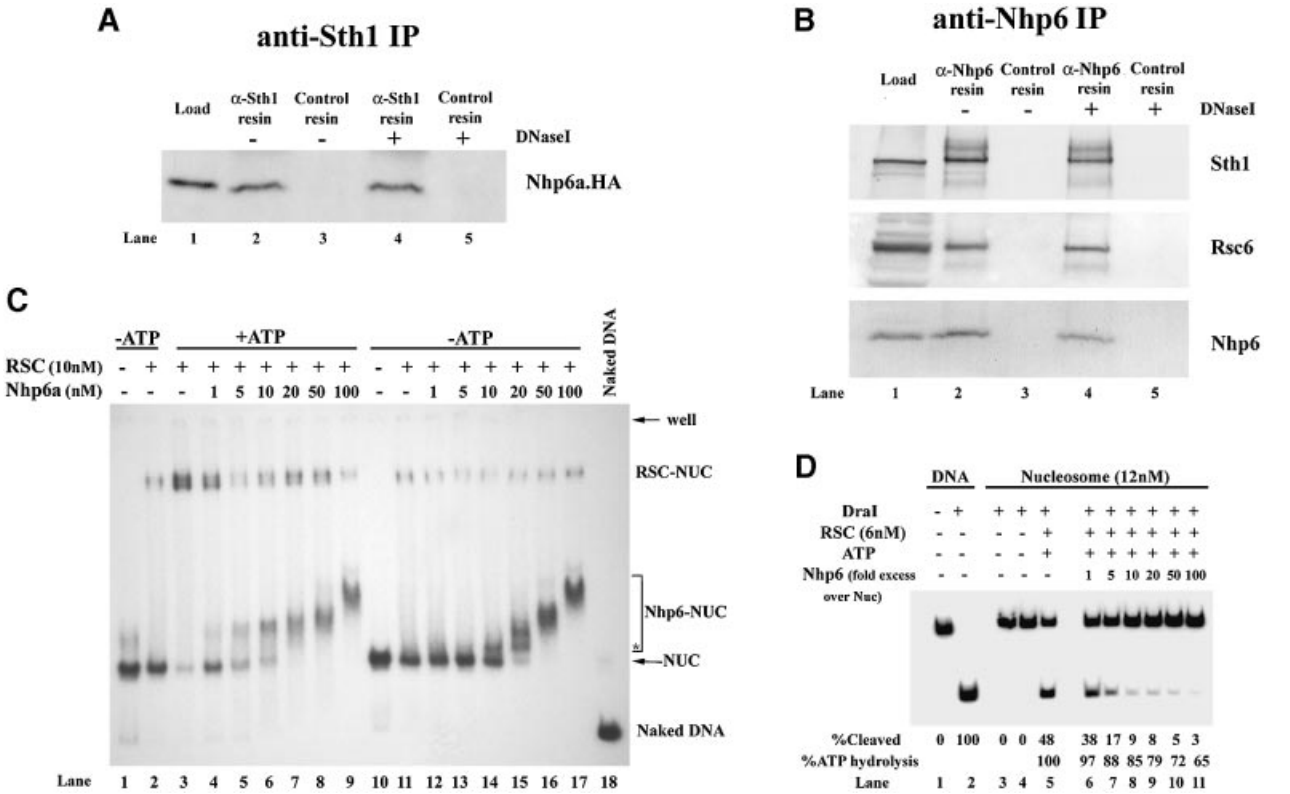


**Fig. 7.** RSC interacts with Nhp6a and facilitates its binding to nucleosomes. (**A**) Nhp6a co-immunoprecipitates Sth1. Immune complexes were formed with anti-Sth1 antibodies and whole-cell extract (from YBC1330, which expresses a chromosomal HA-tagged version of Nhp6a), treated with DNase I (30 units) (lanes 4 and 5; mock, lanes 2 and 3), washed, immunoblotted and probed with anti-HA antibody. Load, 2% of total; pellet, 100%. (**B**) RSC interacts with Nhp6a in the absence of Arp7 and Arp9. Whole-cell extract (1 mg) from an *arp7*Δ *arp9*Δ *mra1* strain (YBC395) was incubated with conjugated anti-Nhp6 resin, treated with DNase I (30 U) (lanes 4 and 5; mock, lanes 2 and 3), washed (250 mM NaCl), immunoblotted, separated by SDS–PAGE and probed with anti-Sth1, anti-Rsc6 or anti-Nhp6. Load, 2% of total; pellet, 100%. (**C**) RSC loads Nhp6a onto nucleosomes. RSC (10 nM) was incubated with nucleosomes (1 nM) and Nhp6a (as indicated) for 20 min and resolved as described in Materials and methods. *The first species formed with Nhp6a only in the absence of ATP, which may represent binding to the exposed linker. (**D**) Nhp6a inhibits access to the *Dra*I site on nucleosomes. Nhp6a was titrated into remodeling reactions (see Figure 5D; Materials and methods).

function as heterodimeric modules in these complexes as well.

### *New models for ARP/ARP and ARP/actin heterodimers*

The central question is: why ARPs and actin are present in two different types of chromatin-regulating complexes, HATs and remodelers? Though our work is limited to Arp7/9 function in RSC under the conditions tested, it does not support a role for nuclear ARPs in promoting DNA-dependent ATPase activity, translocation, histone binding, nucleosome remodeling or RSC complex stability, functions which have been proposed previously for nuclear ARPs (Boyer and Peterson, 2000; Galarneau *et al*., 2000; Olave *et al*., 2002). However, we caution that other ARPs in either yeast or metazoans could possess specialized functions.

Still, based on their similarity, it seems reasonable to propose that ARPs and actin could share certain properties. One attractive model suggests that actin (and possibly Baf53) in human SWI/SNF (BAF) complex binds the ends of actin filaments, effectively capping them (Olave *et al*., 2002; Rando *et al*., 2002). Alternatively, Baf53 or the actin monomer could be involved in actin filament generation. Another simple model for ARP and actin function could involve a common uncharacterized nuclear interaction partner, with Mra1 among a list of candidates. However, based on our observation of ARP heterodimerization, we propose an alternative model that may unify nuclear ARP and actin function. We speculate that ARP/ARP and ARP/actin dimer modules from two different complexes (i.e. a remodeler and a HAT complex) might interact to form a tetramer that bridges the two complexes, one structurally similar to a tetramer segment of an actin filament but bearing two (or three) ARPs. Here, one pair on one complex may mimic the barbed end of an actin filament (as does Arp2/Arp3), whereas the pair on the other complex may mimic the pointed end. The remodeler and HAT complexes would serve to 'cap' the tetramer filament, preventing filament extension from either end. One attractive feature of the model is that it would enable HAT and remodeler complexes to interact and cooperate on a single promoter. In keeping with the genetic data presented here, such interactions might be facilitated by architectural transcription factors like Nhp6, and might only occur in the proper context of chromatin.

### *ARP–NHP6 cooperativity*

Our genetic suppression results, triple mutant combinations and physical interactions support a role for ARPs

**Table III.** *Saccharomyces cerevisiae* strains

| Strain[a] | Genotype | | Source |
|---|---|---|---|
| BCY211 | *MAT***a** | *RSC2.TAP::TRP1 pep4::HIS3 prb1::LEU2 prc1::HISG can1 ade2 trp1 ura3 his3 leu2-3,112* | Saha *et al.* (2002) |
| BCY 330 | *MAT***a**/α | *arp9Δ::LEU2/ ARP9 ura3-1/ura3-1 can1-100/can1-100 ade2-1/ade2-1 trp1-1/trp1-1 leu2-3,112/leu2-3,112 his3-15/his3-15* | Cairns *et al.* (1998) |
| BCY 366 | *MAT***a**/α | *arp7Δ::TRP1/ARP7 ura3-1/ura3-1 can1-100/can1-100 ade2-1/ade2-1 trp1-1/trp1-1 leu2-3,112/leu2-3,112 his3-15/his3-15* | This work |
| BCY 393 | *MAT*α | *ade2-1 trp1-1 can1-100 leu2-3,112 his3-15 ura3-1 arp7Δ::TRP1 arp9Δ::LEU2* | This work |
| BCY 395 | *MAT*α | *ade2-1 trp1-1 can1-100 leu2-3,112 his3-15 ura3-1 arp7Δ::TRP1 arp9Δ::LEU2 mra1* | This work |
| BCY 405 | *MAT***a** | *ade2-1 trp1-1 can1-100 leu2-3,112 his3-15 ura3-1* | This work |
| BCY 426 | *MAT*α | *ade2-1 trp1-1 can1-100 leu2-3,112 his3-15 ura3-1 arp9Δ::LEU2 mra1* | This work |
| BCY 427 | *MAT***a** | *ade2-1 trp1-1 can1-100 leu2-3,112 his3-15 ura3-1 arp7Δ::TRP1 mra1* | This work |
| BCY 430 | *MAT*α | *ade2-1 trp1-1 can1-100 leu2-3,112 his3-15 ura3-1 mra1* | This work |
| YBC27 | *MAT*α | *his4-912δ lys2-128δ leu2Δ1 ura3-52 snf2Δ::LEU2* | This work |
| YBC79 | *MAT***a** | *lys2-128δ leu2Δ1 ura3-52 trp1Δ63 his3Δ200 rsc2Δ::LEU2* | Cairns *et al.* (1999) |
| YBC605 | *MAT***a** | *his3Δ200 leu2Δ0 met15Δ0 trp1Δ63 ura3Δ0* | Cairns *et al.* (1999) |
| YBC775 | *MAT***a** | *lys2-128δ leu2Δ1 ura3-52 trp1Δ63 his3Δ200 arp9Δ::LEU2 [p678; arp9ΔC; CEN TRP1]* | Cairns *et al.* (1998) |
| YBC776 | *MAT*α | *leu2Δ1 ura3-52 trp1Δ63 lys2-128δ his4-912δ arp7Δ::LEU2 [p686; arp7E411K; CEN TRP1]* | Cairns *et al.* (1998) |
| YBC778 | *MAT*α | *leu2Δ1 ura3-52 trp1Δ63 lys2-128δ his4-912δ arp7Δ::LEU2 [p688; arp7G330R; CEN TRP1]* | Cairns *et al.* (1998) |
| YBC786 | *MAT*α | *leu2Δ1 ura3-52 trp1Δ63 lys2-128δ his4-912δ arp7Δ::LEU2 [p684; arp7ΔC1; CEN TRP1]* | Cairns *et al.* (1998) |
| YBC787 | *MAT*α | *leu2Δ1 ura3-52 trp1Δ63 lys2-128δ his4-912δ arp7Δ::LEU2 [p682; arp7A19P; CEN TRP1]* | Cairns *et al.* (1998) |
| YBC788 | *MAT*α | *leu2Δ1 ura3-52 trp1Δ63 lys2-128δ his4-912δ arp7Δ::LEU2 [p683;arp7S33F; CEN TRP1]* | Cairns *et al.* (1998) |
| YBC840 | *MAT***a** | *lys2-128δ leu2Δ1 ura3-52 trp1Δ63 his3Δ200 rsc3Δ::HIS3 [p744;.rsc3-1; CEN LEU2]* | Angus-Hill *et al.* (2001) |
| YBC842 | *MAT***a** | *lys2-128δ leu2Δ1 ura3-52 trp1Δ63 his3Δ200 rsc3Δ::HIS3 [p746; rsc3-2; CEN LEU2]* | Angus-Hill *et al.* (2001) |
| YBC906 | *MAT***a** | *lys2-128δ leu2Δ1 ura3-52 trp1Δ63 his3Δ200 rsc3Δ::HIS3 [p817; rsc3-3; CEN LEU2]* | Angus-Hill *et al.* (2001) |
| YBC928 | *MAT***a** | *lys2-128δ leu2Δ1 ura3-52 trp1Δ63 his3Δ200 pep4Δ::KANMX* | This work |
| YBC944 | *MAT***a** | *lys2-128δ leu2Δ1 ura3-52 trp1Δ63 his3Δ200 sth1Δ::HIS3 [p858;sth1-3 (S806L,T881M); CEN URA3]* | This work |
| YBC946 | *MAT***a** | *lys2-128δ leu2Δ1 ura3-52 trp1Δ63 his3Δ200 sth1Δ::HIS3 [p860;sth1-2 (P646L); CEN URA3]* | This work |
| YBC1156 | *MAT***a** | *ura3-52 trp1Δ63 leu2Δ1 his3 rsc9-1* | Damelin *et al.* (2002) |
| YBC1196 | *MAT*α | *lys2-128δ leu2Δ1 ura3-52 trp1Δ63 his3Δ200 sth1BDΔ3XHA::HIS3MX6* | This work |
| YBC1304 | *MAT***a** | *met15Δ0 lys2Δ0 leu2Δ0 ura3Δ0 his3Δ1 nhp6aΔ::KANMX nhp6bΔ::KANMX* | This work |
| YBC1305 | *MAT*α | *leu2Δ0 ura3Δ0 his3Δ1 lys2Δ0 nhp6aΔ::KANMX nhp6bΔ::KANMX* | This work |
| YBC1307 | *MAT*α | *met15Δ0 leu2Δ0 ura3Δ0 his3Δ1 lys2Δ0 nhp6aΔ::KANMX nhp6bΔ::KANMX* | This work |
| YBC1330 | *MAT***a** | *his3Δ200 leu2Δ0 met15Δ0 trp1Δ63 ura3Δ0 NHP6A.3XHA::HIS3* | This work |
| YBC1515 | *MAT***a** | *his4-912δ lys2 leu2Δ ura3 nhp6aΔ::KANMX nhp6bΔ::KANMX snf2Δ::LEU2* | This work |
| YBC1517 | *MAT*α | *leu2Δ his3Δ lys2 ura3 nhp6aΔ::KANMX nhp6bΔ::KANMX sth1Δ::HIS3 [p858;sth1-3 (S806L,T881M); CEN URA3]* | This work |
| YBC1520 | *MAT*α | *leu2Δ ura3 his3Δ lys2 nhp6aΔ::KANMX nhp6bΔ::KANMX sth1Δ::HIS3 [p860;sth1-2 (P646L); CEN URA3]* | This work |
| YBC1525 | *MAT*α | *leu2Δ ura3 his3Δ lys2 trp1Δ63 nhp6aΔ::KANMX nhp6bΔ::KANMX arp9Δ::LEU2 [p109; ARP9 2μ URA3], [p678; arp9ΔC; CEN TRP1]* | This work |
| YBC1526 | *MAT*α | *leu2Δ ura3 his3Δ lys2 trp1Δ63 nhp6aΔ::KANMX nhp6bΔ::KANMX arp9Δ::LEU2 [p109; ARP9 2μ URA3], [p1014; arp9 G337F G338L; CEN TRP]* | This work |
| YBC1533 | *MAT*α | *leu2Δ1 ura3-52 trp1Δ63 lys2-128Δ his4-912δ arp7Δ::LEU2 [p104; ARP7; CEN TRP1]* | This work |
| YBC1534 | *MAT*α | *leu2Δ1 ura3-52 trp1Δ63 lys2-128Δ his4-912δ arp7Δ::LEU2 [p994; arp7ΔC2; CEN TRP1]* | This work |
| YBC1535 | *MAT***a** | *lys2-128δ leu2Δ1 ura3-52 trp1Δ63 his3Δ200 arp9Δ::LEU2 [p100;ARP9; CEN TRP1]* | This work |
| YBC1536 | *MAT***a** | *lys2-128δ leu2Δ1 ura3-52 trp1Δ63 his3Δ200 arp9Δ::LEU2 [p1014; arp9 G337F G338L; CEN TRP1]* | This work |
| YBC1551 | *MAT*α | *his3Δ200 lys2-801 leu2-3,112 ura3-52 swh3-ts21* | Treich *et al.* (1998) |
| YBC1552 | *MAT*α | *his3Δ200 lys2-801 leu2-3,112 ura3-52 swh3-ΔC* | Treich *et al.* (1998) |
| YBC1621 | *MAT*α | *ura3 trp1Δ63 leu2Δ his3 lys2Δ0 nhp6aΔ::KANMX nhp6bΔ::KANMX rsc9-1 [p1253; NHP6A 2μ URA3]* | This work |

[a]BCY strains and YBC strains are derivatives of the W303 and S288C genetic backgrounds, respectively.

and Nhp6 function in promoter architecture. These results extend the work of others who have made connections between HMG proteins and chromatin. Higher eukaryotes appear to bear an 'on-board' HMG protein; hSWI/SNF contains Baf57 (Wang *et al.*, 1998) and the *Drosophila* BRM complex contains Bap111 (Papoulas *et al.*, 2001). Interestingly, recent studies in mammalian cells have revealed promoter-specific roles for Baf57 in gene activation (Chi *et al.*, 2002). In *Drosophila*, *bap111* deficiencies enhance *brm* mutant phenotypes *in vivo* (Papoulas *et al.*, 2001), which might be analogous to the relationship between *nhp6* and *rsc* mutants. Nhp6 itself has demonstrated roles in promoter architecture at *Pol*II genes such as *CHA1* and *HO*, and microarray analysis of *nhp*ΔΔ mutants and *swi/snf* mutants show partial overlap (Moreira and Holmberg, 2000; Sudarsanam *et al.*, 2000; Yu *et al.*, 2000). We note that the absence of Nhp6a/b does not impact *ARP7* or *ARP9* expression (Moreira and Holmberg, 2000). In addition, Nhp6 proteins function in activation of the *Pol*III *SNR6* gene (Kruppa *et al.*, 2001; Lopez *et al.*, 2001). Though RSC is present at *Pol*III genes (Ng *et al.*, 2002), we observe no suppression of *arp* mutant temperature sensitivity by multicopy *BRF1* or *PFC-1*, both characterized suppressors of *nhp6* mutations at *SNR6*, suggesting that a reduction in *Pol*III transcription is not the sole defect in *arp* mutants (data not shown). Recent studies of the yeast SPN (Spt16-Pob3-Nhp6) complex (Brewster *et al.*, 2001; Formosa *et al.*, 2001) provide genetic and biochemical evidence for Nhp6 interaction with Spt16-Pob3 that is similar conceptually to our observations with RSC. Taken together, HMG proteins are emerging as versatile factors that interact and cooperate

functionally with different transcription complexes to promote complex interactions, though much remains to be learned about their coordinated functions.

### RSC facilitates the binding of Nhp6a to nucleosomes

Here, we show that RSC action promotes the binding of Nhp6a to nucleosomal DNA, with a concomitant reduction in access to the nucleosomal *Dra*I site. These results relate to very recent experiments with the *Drosophila* HMGB1 and the chromatin remodeling factor ACF, which contains the remodeling ATPase ISWI (Bonaldi *et al*., 2002). HMGB1 contains two HMG domains as well as a C-terminal extension that greatly reduces DNA affinity. An HMGB1 derivative lacking its C-terminus (HMGB1ΔC) binds DNA with high affinity, similar to Nhp6a. Interestingly, HMGB1 facilitates nucleosome sliding by ACF, possibly by assisting the binding of ACF to bent DNA at the location where DNA enters/exits the nucleosome, whereas HMGB1ΔC inhibits sliding; with its 100-fold higher affinity, it may block binding by ACF (Bonaldi *et al*., 2002). We find that Nhp6a, like HMGB1ΔC, also blocks an aspect of remodeling, access to the *Dra*I site (Figure 7D). This is probably due (in part) to blocking RSC-nucleosome interactions, as the ATP-dependent recognition of the nucleosome by RSC is reduced in the presence of Nhp6a, even at an Nhp6a-to-nucleosome ratio of 1:1 (Figure 7C, compare lanes 3 and 4). Interestingly, despite this reduction in RSC–nucleosome interaction, RSC facilitates the binding of Nhp6a. Therefore, another basis for reduced *Dra*I access is probably due to Nhp6a binding at or near the *Dra*I site, following its loading by RSC.

One model for RSC action involves the creation of negatively twisted DNA waves, which are initiated by ATP-dependent DNA translocation by the remodeler ATPase near the entry/exit site, and then propagate around the nucleosome to enable factor binding and/or nucleosome sliding (Saha *et al*., 2002). In keeping with this model, Nhp6a strongly prefers bent and undertwisted DNA (Allain *et al*., 1999), predicted properties of the wave intermediate. However, additional experiments are required to understand fully the interplay between remodelers and HMG proteins.

In conclusion, our data are consistent with a model where RSC helps load Nhp6a onto nucleosomes at certain promoters, and that ARP proteins utilize their actin-related regions to form heterodimers that work with Nhp6a and other factors to achieve proper promoter architecture.

## Materials and methods

### Media, genetic methods and strains

Standard procedures were used for media preparations, transformations, sporulation and tetrad analysis. All strains are derivatives of S288C, except those bearing *arp*Δ or *mra1* mutations, which are derivatives of W303. Strain identities are provided in the figure legends, and full genotypes are listed in Table III.

### Plasmids

All PCR primer sequences are available on request. The Arp7–Arp9 bicistronic expression plasmid consists of a ribosomal binding site (RBS) and flanking restrictions sites (*Xba*I, *Bam*HI, RBS, *Nde*I, *Bgl*II and *Hind*III, a gift from C.Hill's laboratory) cloned into pET29a (Novagen) via *Xba*I–*Hind*III to create p988. PCR-generated open reading frames (ORFs) of *Arp7*.7XHIS and Flag.*Arp9* were cloned into p988 to create p993 (p1329 for Arp7ΔC/Arp9ΔC). Plasmids for galactose-regulated expression in yeast are derivatives of the pRSGAL1 series. For full-length *ARP7*.7XHIS (p1158), a *Bam*HI–*Xho*I fragment from p990 was cloned into p423*GAL1*. Plasmid *arp7ΔC*.7XHIS (p1274) places a 7Xhistidine epitope at position 436. The PCR fragment was then subcloned into p1158 via *Afl*II–*Xho*I double digest, isolation and ligation. To prepare Flag.*Arp9* (p1272), a *Bam*HI–*Xho*I fragment from p992 was subcloned into p424GAL1. The plasmid Flag.*arp9ΔC* (p1273) introduces a Flag epitope at the N-terminus, eliminates intronic sequences and introduces a stop codon at amino acid 438.

Plasmids bearing site-directed mutations in *ARP7* or *ARP9* were prepared using the Quick Change method (Stratagene) and were subcloned and sequenced. For generation of *arpΔC2* mutations, primers were designed to generate two stop codons (at amino acid positions 436 and 437) followed by a frame shift mutation. For the isolation of *arp9-1,* a PCR-generated library of *arp9* G337X G338X mutations (where X is a random amino acid) was transformed into YBC86 (*arp9*Δ), plated on medium containing 5-fluoro-orotic acid (5-FOA) to enforce loss of the YEp24.*ARP9 URA3* and then screened for loss of viability at 38°C. *arp9-1* is one of many isolates that conferred a $Ts^-$ phenotype.

### Extract preparation and immunoprecipitation

Yeast extracts were prepared as described previously (Cairns *et al*., 1999). For temperature shifts, cultures were split while in logarithmic growth at 30°C and continued at permissive or non-permissive temperatures (as indicated) for 2.5 doublings. For galactose induction experiments, YBC928 transformants were grown in selective media (with 1.5% Raffinose) to mid-logarithmic phase, galactose (1% final) was added and growth continued for 4–8 h at 22–30°C.

For coassembly experiments, anti-Arp7, anti-Arp9, anti-Sth1 and anti-Swi3 antibodies were conjugated to protein A beads, incubated for 2 h with whole-cell extracts (400 μg) derived from WT, *mra1* and *arp* mutants (BCY405, BCY426, BCY427, BCY430), washed twice with IP buffer [50 mM Tris–Cl pH 7.7, 1 mM EDTA, 0.05% Tween-20, 10% (v/v) glycerol] containing 250 mM NaCl and eluted with 6 M urea.

### Purification of Arp7/Arp9 heterodimer and Nhp6a

BL21 Codon (+) cells (Stratagene) harboring p993 were grown under standard conditions, induced with 1 mM ispropyl-β-D-thiogalactopyranoside (IPTG) at an $OD_{600}$ of 0.3 and harvested at $OD_{600}$ of 1.0 after 3 h. Cells were pelleted, resuspended in buffer B (50 mM $NaH_2PO_4$ pH 8.0, 10% glycerol, 1 mM β-ME and 0.1% NP40) containing 100 mM KCl, sonicated, clarified at 10 000 *g* (25 min) and bound to Ni-NTA agarose (Qiagen) for 2 h at 4°C. The beads were washed with buffer B containing 450 mM KCl and eluted in buffer B containing 200 mM KCl and 200 mM imidazole pH 8.0. The eluate was incubated with anti-Flag M2-agarose (Sigma) for 2 h at 4°C, washed with buffer B containing 450 mM KCl and eluted with the addition of Flag peptide (Sigma) at 100 ng/μl. Nhp6a was purified from *E.coli* as described previously (Formosa *et al*., 2001).

### RSCΔ7/9 functional analysis

WT RSC was purified from strain BCY211, which expresses TAP-tagged (Puig *et al*., 2001) Rsc2 from the chromosomal *RSC2* promoter as described previously (Saha *et al*., 2002). RSCΔ7/9 was purified from YBC395 (*mra1-1 arp7*Δ *arp9*Δ) harboring *pTAP.RSC2* (p1003), a plasmid directing expression of TAP-tagged Rsc2 by the same procedure as WT RSC. DNA-dependent ATPase activity, triple-helix displacement assays and remodeling reactions were done as described previously (Saha *et al*., 2002).

### Reconstitution experiments

The Arp7/Arp9 dimer was purified from yeast extracts derived from galactose-induced expression of Arp7.7XHIS and Flag.Arp9 (and their derivatives). Extract (3–6 mg) was bound to Ni-NTA agarose (Qiagen) in IP Buffer (with 100 mM NaCl), washed with IP Buffer (250 mM NaCl) and eluted in IP buffer containing 150 mM NaCl and 200 mM imidazole pH 8.0. The eluate (250 ng of Arp7/9 complex) was immobilized on anti-Flag M2 agarose (Sigma), washed (IP buffer with 200 mM NaCl) and incubated with 500 ng of RSCΔ7/9 or WT RSC. Reactions were incubated for 1 h at 4°C, washed with IP buffer containing 500 mM NaCl and eluted with 3X Flag peptide (Sigma) at 150 ng/μl.

### Mobility shift analysis

RSC-nucleosome–Nhp6 binding reactions (5 μl) contained 20 mM Tris–acetate pH 7.9, 6% (w/v) glycerol, 10 mM MgOAc, 50 mM KOAc, 1 mM dithiothreitol (DTT) and 0.1 mg/ml BSA, with or without 1 mM

ATP. Reactions were incubated at 30°C for 20 min and species were separated (4 h at 150 V) on a native 3.2% polyacrylamide gel (acryl:bis of 38.9:1.1) in 10 mM Tris–Cl pH 8.0 and 1 mM EDTA at 4°C with buffer circulation.

## Acknowledgements

We thank David Stillman and Ian Willis for plasmids, Tim Formosa for anti-Nhp6 antiserum and expression construct, Brehon Laurent for *sth1* alleles and plasmids, Andreas Forster and Chris Hill for the bicistronic *E.coli* expression vector, Marian Carlson for *rsc8/swh3* strains, Bob Schackmann for oligonucleotide synthesis, Jacqui Wittmeyer for nucleosomes, Alisha Schlichter for the RSC2.TAP plasmid and bromodomain deletion strain, Andy VanDemark for help with PYMOL, and Tim Formosa, Jacqui Wittmeyer, Don Ayer, Margaret Kasten, Mat Gordon and David Stillman for comments on the manuscript. This work was funded by the National Institutes of Health (GM60415 to B.R.C.; CA24014 for core facilities) and the Howard Hughes Medical Institute. B.R.C. is an Assistant Investigator with the Howard Hughes Medical Institute and an Investigator at the Huntsman Cancer Institute.

## References

Allain,H.-T., Yen,Y.M., Masse,J.E., Schultze,P., Dieckmann. T., Johnson,R. and Feigon,J. (1999) Solution structure of the HMG protein NHP6A and its interaction with DNA reveals the structural determinants for non-sequence-specific binding. *EMBO J.*, **18**, 2563–2579.

Angus-Hill,M.L., Schlichter,A., Roberts,D., Erdjument-Bromage,H., Tempst,P. and Cairns,B.R. (2001) A Rsc3–Rsc30 zinc cluster heterodimer reveals new roles for the chromatin remodeling complex RSC in gene expression and cell cycle control. *Mol. Cell*, **7**, 741–751.

Bonaldi,T., Langst,G., Strohner,R., Becker,P.B. and Bianchi,M.E. (2002) The DNA chaperone HMGB1 facilitates ACF/CHRAC-dependent nucleosome sliding. *EMBO J.*, **21**, 6865–6873.

Boyer,L.A. and Peterson,C.L. (2000) Actin-related proteins (Arps): conformational switches for chromatin- remodeling machines? *BioEssays*, **22**, 666–672.

Brewster,N.K., Johnston,G.C. and Singer,R.A. (2001) A bipartite yeast SSRP1 analog comprised of Pob3 and Nhp6 proteins modulates transcription. *Mol. Cell Biol.*, **21**, 3491–3502.

Cairns,B.R. (1998) Chromatin remodeling machines: similar motors, ulterior motives. *Trends Biochem. Sci.*, **23**, 20–25.

Cairns,B.R. *et al*. (1996) RSC, an essential, abundant chromatin-remodeling complex. *Cell*, **87**, 1249–1260.

Cairns,B.R., Erdjument-Bromage,H., Tempst,P., Winston,F. and Kornberg,R.D. (1998) Two actin-related proteins are shared functional components of the chromatin-remodeling complexes RSC and SWI/SNF. *Mol. Cell*, **2**, 639–651.

Cairns,B.R., Schlichter,A., Erdjument-Bromage,H., Tempst,P., Kornberg,R.D. and Winston,F. (1999) Two functionally distinct forms of the RSC nucleosome-remodeling complex, containing essential AT hook, BAH, and bromodomains. *Mol. Cell*, **4**, 715–723.

Chi,T.H., Wan,M., Zhao,K., Taniuchi,I., Chen,L., Littman,D.R. and Crabtree,G.R. (2002) Reciprocal regulation of CD4/CD8 expression by SWI/SNF-like BAF complexes. *Nature*, **418**, 195–199.

Costigan,C., Kolodrubetz,D. and Snyder,M. (1994) NHP6A and NHP6B, which encode HMG1-like proteins, are candidates for downstream components of the yeast SLT2 mitogen-activated protein kinase pathway. *Mol. Cell Biol.*, **14**, 2391–2403.

Damelin,M. *et al*. (2002) The genome-wide localization of Rsc9, a component of the RSC chromatin-remodeling complex, changes in response to stress. *Mol. Cell*, **9**, 563–573.

Formosa,T., Eriksson,P., Wittmeyer,J., Ginn,J., Yu,Y. and Stillman,D.J. (2001) Spt16-Pob3 and the HMG protein Nhp6 combine to form the nucleosome-binding factor SPN. *EMBO J.*, **20**, 3506–3517.

Galarneau,L. *et al*. (2000) Multiple links between the NuA4 histone acetyltransferase complex and epigenetic control of transcription. *Mol. Cell*, **5**, 927–937.

Gavin,A.C. *et al*., (2002) Functional organization of the yeast proteome by systematic analysis of protein complexes. *Nature*, **415**, 141–147.

Harata,M., Oma,Y., Mizuno,S., Jiang,Y.W., Stillman,D.J. and Wintersberger,U. (1999) The nuclear actin-related protein of *Saccharomyces cerevisiae*, Act3p/Arp4, interacts with core histones. *Mol. Biol. Cell*, **10**, 2595–2605.

Havas,K., Whitehouse,I. and Owen-Hughes,T. (2001) ATP-dependent chromatin remodeling activities. *Cell. Mol. Life Sci.*, **58**, 673–682.

Ikura,T., Ogryzko,V.V., Grigoriev,M., Groisman,R., Wang,J., Horikoshi,M., Scully,R., Qin,J. and Nakatani,Y. (2000) Involvement of the TIP60 histone acetylase complex in DNA repair and apoptosis. *Cell*, **102**, 463–473.

Jiang,Y.W. and Stillman,D.J. (1996) Epigenetic effects on yeast transcription caused by mutations in an actin-related protein present in the nucleus. *Genes Dev.*, **10**, 604–619.

Kabsch,W. and Holmes,K.C. (1995) The actin fold. *FASEB J.*, **9**, 167–174.

Kabsch,W., Mannherz,H.G., Suck,D., Pai,E.F. and Holmes,K.C. (1990) Atomic structure of the actin:DNase I complex. *Nature*, **347**, 37–44.

Kruppa,M., Moir,R.D., Kolodrubetz,D. and Willis,I.M. (2001) Nhp6, an HMG1 protein, functions in SNR6 transcription by RNA polymerase III in *S. cerevisiae*. *Mol. Cell*, **7**, 309–318.

Lopez,S., Livingstone-Zatchej,M., Jourdain,S., Thoma,F., Sentenac,A. and Marsolier,M.C. (2001) High-mobility-group proteins NHP6A and NHP6B participate in activation of the RNA polymerase III SNR6 gene. *Mol. Cell Biol.*, **21**, 3096–3104.

Machesky,L.M. and May,R.C. (2001) Arps: actin-related proteins. *Results Probl. Cell Differ.*, **32**, 213–229.

May,R.C. (2001) The Arp2/3 complex: a central regulator of the actin cytoskeleton. *Cell. Mol. Life Sci.*, **58**, 1607–1626.

Moreira,J.M. and Holmberg,S. (2000) Chromatin-mediated transcriptional regulation by the yeast architectural factors NHP6A and NHP6B. *EMBO J.*, **19**, 6804–6813.

Narlikar,G.J., Fan,H.Y. and Kingston,R.E. (2002) Cooperation between complexes that regulate chromatin structure and transcription. *Cell*, **108**, 475–487.

Ng,H.H., Robert,F., Young,R.A. and Struhl,K. (2002) Genome-wide location and regulated recruitment of the RSC nucleosome-remodeling complex. *Genes Dev.*, **16**, 806–819.

Olave,I.A., Reck-Peterson,S.L. and Crabtree,G.R. (2002) Nuclear actin and actin-related proteins in chromatin remodeling. *Annu. Rev. Biochem.*, **71**, 755–781.

Papoulas,O., Beek,S.J., Moseley,S.L., McCallum,C.M., Sarte,M., Shearn,A. and Tamkun,J.W. (1998) The *Drosophila* trithorax group proteins BRM, ASH1 and ASH2 are subunits of distinct protein complexes. *Development*, **125**, 3955–3966.

Papoulas,O., Daubresse,G., Armstrong,J.A., Jin,J., Scott,M.P. and Tamkun,J.W. (2001) The HMG-domain protein BAP111 is important for the function of the BRM chromatin-remodeling complex *in vivo*. *Proc. Natl Acad. Sci. USA*, **98**, 5728–5733.

Park,J., Wood,M.A. and Cole,M.D. (2002) BAF53 forms distinct nuclear complexes and functions as a critical c-Myc-interacting nuclear cofactor for oncogenic transformation. *Mol. Cell Biol.*, **22**, 1307–1316.

Paull,T.T., Carey,M. and Johnson,R.C. (1996) Yeast HMG proteins NHP6A/B potentiate promoter-specific transcriptional activation *in vivo* and assembly of preinitiation complexes *in vitro*. *Genes Dev.*, **10**, 2769–2781.

Peterson,C.L., Zhao,Y. and Chait,B.T. (1998) Subunits of the yeast SWI/SNF complex are members of the actin-related protein (ARP) family. *J. Biol. Chem.*, **273**, 23641–23644.

Phelan,M.L., Sif,S., Narlikar,G.J. and Kingston,R.E. (1999) Reconstitution of a core chromatin remodeling complex from SWI/SNF subunits. *Mol. Cell*, **3**, 247–253.

Poch,O. and Winsor,B. (1997) Who's who among the *Saccharomyces cerevisiae* actin-related proteins? A classification and nomenclature proposal for a large family. *Yeast*, **13**, 1053–1058.

Puig,O., Caspary,F., Rigaut,G., Rutz,B., Bouveret,E., Bragado-Nilsson,E., Wilm,M. and Seraphin,B. (2001) The tandem affinity purification (TAP) method: a general procedure of protein complex purification. *Methods*, **24**, 218–229.

Rando,O.J., Zhao,K., Janmey,P. and Crabtree,G.R. (2002) Phosphatidylinositol-dependent actin filament binding by the SWI/SNF-like BAF chromatin remodeling complex. *Proc. Natl Acad. Sci. USA*, **99**, 2824–2829.

Robinson,R.C., Turbedsky,K., Kaiser,D.A., Marchand,J.B., Higgs,H.N., Choe,S. and Pollard,T.D. (2001) Crystal structure of Arp2/3 complex. *Science*, **294**, 1679–1684.

Saha,A., Wittmeyer,J. and Cairns,B.R. (2002) Chromatin remodeling by RSC involves ATP-dependent DNA translocation. *Genes Dev.*, **16**, 2120–2134.

Schafer,D.A. and Schroer,T.A. (1999) Actin-related proteins. *Annu. Rev. Cell. Dev. Biol.*, **15**, 341–363.

Shen,X., Mizuguchi,G., Hamiche,A. and Wu,C. (2000) A chromatin remodelling complex involved in transcription and DNA processing. *Nature*, **406**, 541–544.

Sudarsanam,P., Iyer,V.R., Brown,P.O. and Winston,F. (2000) Whole-genome expression analysis of snf/swi mutants of *Saccharomyces cerevisiae*. *Proc. Natl Acad. Sci. USA*, **97**, 3364–3369.

Treich,I., Ho,L. and Carlson,M. (1998) Direct interaction between Rsc6 and Rsc8/Swh3,two proteins that are conserved in SWI/SNF-related complexes. *Nucleic Acids Res.*, **26**, 3739–3745.

Vignali,M., Hassan,A.H., Neely,K.E. and Workman,J.L. (2000) ATP-dependent chromatin-remodeling complexes. *Mol. Cell Biol.*, **20**, 1899–1910.

Volkmann,N. *et al*. (2001) Structure of Arp2/3 complex in its activated state and in actin filament branch junctions. *Science*, **293**, 2456–2459.

Wang,W. *et al*. (1996) Purification and biochemical heterogeneity of the mammalian SWI–SNF complex. *EMBO J.*, **15**, 5370–5382.

Wang,W., Chi,T., Xue,Y., Zhou,S., Kuo,A. and Crabtree,G.R. (1998) Architectural DNA binding by a high-mobility-group/kinesin-like subunit in mammalian SWI/SNF-related complexes. *Proc. Natl Acad. Sci. USA*, **95**, 492–498.

Xue,Y., Canman,J.C., Lee,C.S., Nie,Z., Yang,D., Moreno,G.T., Young,M.K., Salmon,E.D. and Wang,W. (2000) The human SWI/SNF-B chromatin-remodeling complex is related to yeast rsc and localizes at kinetochores of mitotic chromosomes. *Proc. Natl Acad. Sci. USA*, **97**, 13015–13020.

Yu,Y., Eriksson,P. and Stillman,D.J. (2000) Architectural transcription factors and the SAGA complex function in parallel pathways to activate transcription. *Mol. Cell Biol.*, **20**, 2350–2357.

Zhao,K., Wang,W., Rando,O.J., Xue,Y., Swiderek,K., Kuo,A. and Crabtree,G.R. (1998) Rapid and phosphoinositol-dependent binding of the SWI/SNF-like BAF complex to chromatin after T lymphocyte receptor signaling. *Cell*, **95**, 625–636.

*Received October 25, 2002; revised and accepted April 28, 2003*